# Initial nucleation and growth of in-plane solid-liquid-solid silicon nanowires catalyzed by indium

Linwei Yu and Pere Roca i Cabarrocas
*Laboratoire de Physique des Interfaces et des Couches Minces (LPICM), Ecole Polytechnique, CNRS, 91128 Palaiseau, France*
(Received 18 February 2009; revised manuscript received 21 April 2009; published 20 August 2009)

We report a systematic investigation of the initial nucleation and growth of in-plane solid-liquid-solid (IPSLS) silicon nanowires (SiNWs), catalyzed by indium (In) drops prepared *in situ* by a $H_2$ plasma superficial reduction of indium tin oxide in a plasma-enhanced chemical-vapor deposition system. A supersaturation of Si atoms in the In catalyst drop is first established by the absorption of the hydrogenated amorphous silicon (a-Si:H) layer coating the catalyst drops. The initial nucleation of Si seeds in the catalyst drop is found to happen preferentially along the catalyst bottom edge and the lateral growth of SiNW is actually triggered by the largest Si seed that tilts the catalyst drop into the opposite direction to form new absorption edge with nearby a-Si:H layer. We show that the ratio of the a-Si:H layer thickness to the catalyst diameter is a key controlling factor for achieving a high-growth activation rate of the lateral IPSLS-SiNWs.

DOI: 10.1103/PhysRevB.80.085313 PACS number(s): 61.46.Km, 81.07.Vb, 81.16.Dn

Silicon nanowires (SiNWs) can be obtained via different mechanisms, for example, the well-known vapor-liquid-solid (VLS) (Ref. 1) and oxide-assisted growth (Ref. 2) modes, and serve as the key elements for high performance SiNWs-based transistors,[3,4] biosensors,[5,6] and energy harvesting devices.[7,8] Recently, we reported an in-plane solid-liquid-solid (IPSLS) growth mode for fabricating lateral SiNWs in a plasma-enhanced chemical-vapor deposition (PECVD) system during an all-*in situ* process.[9] The indium (In) catalyst drops, covered by a thin hydrogenated amorphous silicon (a-Si:H) layer, are activated into lateral growth during a reacting-gas-free thermal annealing process. This IPSLS growth mode can be viewed as a nanoscale solid-state crystallization process guided by a *moving* In catalyst drop. During the lateral movement, the In catalyst drops absorb the a-Si:H matrix and produce crystalline SiNWs behind. A high growth rate of $\sim 10^2$ nm/s and rich growth dynamics, due to the interplay between the absorption and deposition interfaces, are directly witnessed in real time scanning electron microscopy (SEM) characterizations.[9] While the unique growth mechanism and growth dynamics are of fundamental interest, this IPSLS growth mode renders a rich flexibility in controlling the morphology and position of the produced SiNW, and thus opens new opportunities for various SiNWs-based device applications.

In order to achieve full control over the growth of SiNWs obtained via IPSLS mode, it is crucial to obtain an in-depth understanding of the initial nucleation and growth of the IPSLS-SiNWs, in order to identify the key controlling factors for a high activation rate. In this paper, we focus on the initial nucleation of Si seeds in the In catalyst drop and explore how these crystalline seeds eventually trigger the growth of lateral IPSLS-SiNWs. We show that the ratio of the covering a-Si:H layer thickness to the catalyst diameter is the key parameter that influences the growth activation rate of the IPSLS-SiNW. The major steps involved in the formation of the lateral SiNW are discussed in detail.

The experimental procedure for the growth of IPSLS SiNWs includes three steps: (1) the In catalyst drops are prepared *in situ* by a $H_2$ plasma treatment of an indium tin oxide (ITO) substrate in a PECVD system at 250–350 °C; (2) the substrate is cooled to a temperature below the melting point of In ($T_{In}$=157 °C) and covered with a thin layer of a-Si:H (10–100 nm); (3) the sample is annealed in vacuum (in the same chamber) at substrate temperature of $T_{sub}$ =350–500 °C to activate the lateral growth of the SiNWs. All the fabrication steps can be done in a one-pump-down process. More details about the plasma deposition conditions are provided in our previous work.[9]

A SEM image of a typical IPSLS SiNW and a schematic illustration of the sample structure are presented in Figs. 1(a) and 1(b), respectively. The in-plane growth of the SiNW is guided by an In catalyst drop that consumes the a-Si:H matrix and produces a crystalline SiNW behind, during a thermal annealing at 450 °C for 10 min. The insets in Fig. 1(a) provide enlarged views of the original nucleation site and final end of the SiNW.

Similar to the solid-phase crystallization process of a-Si:H, the nanoscaled crystallization process of the a-Si:H matrix into crystalline SiNWs is driven by the Gibbs energy difference between the amorphous and the crystalline Si phases. The higher Gibbs potential energy in the amorphous a-Si:H matrix ($E_a$) as compared to that in crystalline SiNWs ($E_c$), with $\Delta E_{ac}=E_a-E_c\approx 0.12-0.15$ eV,[10,11] provides the major driving force for the lateral growth of the IPSLS SiNWs. From a kinetics point of view, the In catalyst in the IPSLS growth mode plays an important role to lower the transformation energy barrier in a direct solid-phase-crystallization (amorphous-to-crystalline) process, which arises from the high energy saddle states during the network rearrangement and is $\sim$2.7 eV.[12,13] Meanwhile, in the IPSLS growth mode, the Si atoms are absorbed from solid a-Si:H matrix at the front interface and then transported and deposited at the crystalline SiNW end. The major steps involved in the IPSLS growth mode share much similarity with the well-known VLS process, except that in the VLS mode the feeding precursor is in gas phase.[1,14]

Taking the Gibbs energy of Si atom in crystalline silicon as a reference, as illustrated in Fig. 2, the chemical potential of the dissolved Si atom in an In catalyst ($E_i$ with a concentration of $C_{Si}$) can be given by[15–17]

 

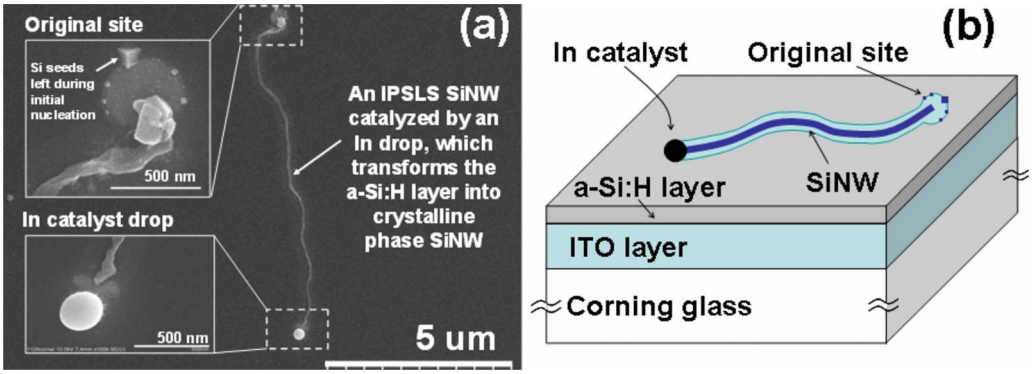


FIG. 1. (Color online) (a) SEM image of a typical SiNW obtained via IPSLS mode. The upper and down insets provide enlarged views of the original site and the final end of the SiNW; (b) schematic illustration of the sample structure and the IPSLS growth mechanism of a lateral SiNW catalyzed by an In drop.

$$\Delta\mu = E_i - E_c = kT \cdot \ln S = kT \cdot \ln(C_{\mathrm{Si}}/C_{eq}^c), \quad (1)$$

where $C_{eq}^c$ is the equilibrium Si concentration at the c-SiNW/In interface and $S \equiv C_{\mathrm{Si}}/C_{eq}^c$ is the supersaturation in the In catalyst while $k$ and $T$ are the Boltzmann constant and the substrate temperature, respectively.

The higher Gibbs energy in the a-Si:H matrix leads to a higher equilibrium Si concentration at the a-Si/In interface than that at the c-Si/In (or SiNW/In) interface,

$$C_{eq}^a = C_{eq}^c \cdot e^{\Delta E_{ac}/kT}, \quad (2)$$

which establishes a supersaturation of dissolved Si atoms with respect to the c-Si/In interface. The maximum supersaturation that can be established (at ~500 °C) in the In catalyst is estimated to be

$$S = C_{\mathrm{Si}}/C_{eq}^c = e^{\Delta\mu/kT} \leq C_{eq}^a/C_{eq}^c = e^{\Delta E_{ac}/kT} \approx 6.1 - 9.5. \quad (3)$$

This supersaturation state enables the nucleation of stable Si seeds in the In catalyst with a critical size of around

$$r_c = 2 \cdot \gamma_{ls} \cdot \Omega_{\mathrm{Si}}/\Delta\mu = 2 \cdot \gamma_{ls} \cdot \Omega_{\mathrm{Si}}/(kT \cdot \ln S) \approx 2.4 - 3.3 \ \mathrm{nm}, \quad (4)$$

where $\gamma_{ls}$ and $\Omega_{\mathrm{Si}}$ are the interface energy between Si seeds and In and the atomic volume of Si, respectively.

The nucleation process is schematically shown in Fig. 3(a). During the thermal annealing, when the substrate temperature increases to $T_{\mathrm{sub}} > T_{\mathrm{In}} = 157$ °C, the In catalyst turns into liquid state and begins to absorb the Si atoms from the covering a-Si:H layer (with a thickness of $H_a$). Therefore, the concentration of Si atoms in the catalyst increases until $C_{\mathrm{Si}} \approx C_{eq}^a$. Then, nucleation of stable Si seeds may happen in the In catalyst and provide nucleation centers for further *heterogeneous* nucleation and growth. It is worth to note that, according to the SEM observations, the formation of Si seeds seems to preferentially happen along the bottom edge of the catalyst drop, at the triple interface between a-Si:H, the ITO layer and the In catalyst. This can be inferred from the SEM images taken in the area of SiNW nucleation, as shown in Fig. 1(a) (upper inset) and Fig. 4(a). It can be seen that a chain of small Si seeds are found along the edge of the *starting pits* left by the catalyst drops. This can be explained by the fact that: the c-Si/In interface energy ($\gamma_{ls}$ on the order of ~1 J/m$^2$) (Ref. 17) is much larger than the energies of the

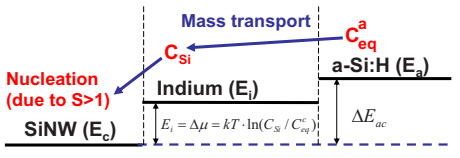


FIG. 2. (Color online) Schematic illustration for the relative Gibbs energy state of Si atoms in the crystalline SiNW ($E_c$), In catalyst solution ($E_i$), and a-Si:H matrix ($E_a$).

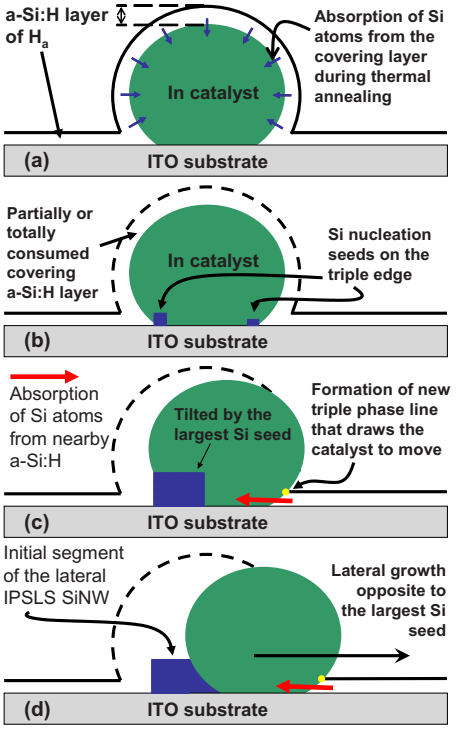


FIG. 3. (Color online) [(a) and (b)] Schematic illustration of the absorption of the covering a-Si:H and initial nucleation of Si seeds in the In catalyst; [(c) and (d)] the nucleation of the lateral IPSLS SiNW triggered by the formation of large Si seed that tilts the catalyst drop to specific direction and forms a new absorption interface with the nearby a-Si:H.

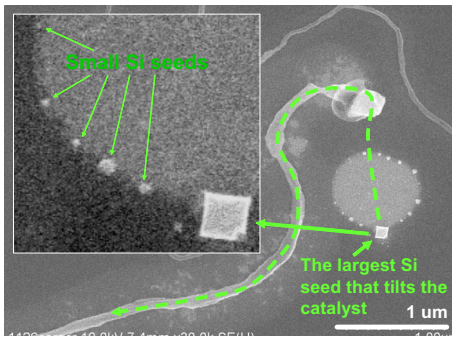


**(a)**

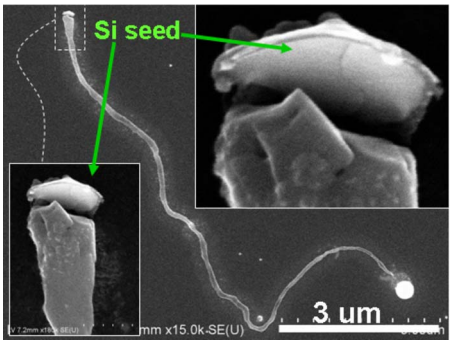


**(b)**

FIG. 4. (Color online) Close views of the original starting site of two lateral SiNWs, where the largest Si seeds on the edge are always opposite to the initial growth direction of the SiNWs but not necessarily connected to the SiNWs.

amorphous-crystalline Si interface ($\gamma_{ac}$) and the oxide (ITO)/Si interface ($\gamma_{oc}$).[18] The effective/average surface energy *seen* by a Si seed at the bottom edge line is

$$\gamma_{eff} = \gamma_{ac} \cdot \alpha_{ac} + \gamma_{oc} \cdot \alpha_{oc} + \gamma_{ls} \cdot (1 - \alpha_{ac} - \alpha_{oc}) < \gamma_{ls} \quad (5)$$

with $\alpha_{ac}$ and $\alpha_{ao}$ being the portion of touching area between Si seed with the a-Si:H and ITO, respectively. Therefore, the nucleation barrier at the sites along the bottom edge (which is $\sim\gamma^2$) (Ref. 15) is generally lower than that inside the catalyst liquid and thus allows for the formation of smaller stable Si seeds first at the bottom edge line (since $r_c \sim \gamma$).

Interestingly, the initial growth direction of the lateral SiNW is always found to be opposite to the largest Si seed, as shown, for instance, in Figs. 1 and 4. These observations suggest that the catalyst drop is actually tilted by the largest Si seed on the catalyst bottom edge into a specific growth direction. As illustrated in Fig. 3(c), once the stable Si seeds are formed along the bottom edge, the largest one will provide the *most stable sink* for the dissolved Si atoms. According to the regular faceting of the largest Si seeds, as shown in Figs. 1 and 4, these seeds are usually terminated by relatively more stable Si(111) and Si(100) planes. When one of the crystalline seeds finally becomes large enough to effectively *tilt* the In drop towards the opposite direction, the liquid catalyst drop has a chance to contact the nearby a-Si:H layer and form a new absorption front there. As discussed in our previous work, this newly formed triple phase line, between the In, a-Si:H, and vacuum media, will exert a drawing force on the liquid catalyst drop.[9] This force, arising from the imbalanced surface tensions at the triple line (due to the continuous absorption of Si atoms at the In/a-Si interface), eventually initiates the lateral growth of IPSLS-SiNW.

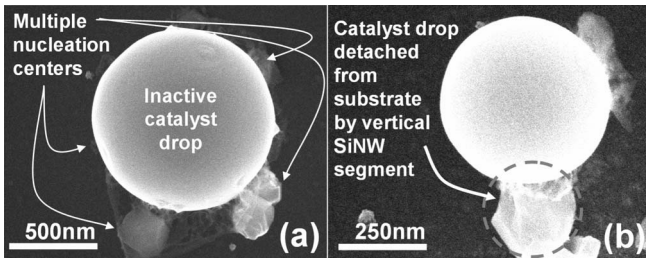


FIG. 5. SEM images of the inactive catalyst drops due to (a) the formation of multiple Si seeds around the bottom edge line or (b) a vertical growth that detaches the catalyst from the substrate.

It is worth to point out that the largest Si seed, which tilts the catalyst drop for lateral movement, is not always the nucleation center for the following growth of lateral SiNWs. In some cases as shown in Figs. 1, 4(a), and 4(b), the newly formed interface with the nearby a-Si:H layer could foster other Si seeds to serve as the nucleation center for the start up of the lateral SiNWs. This situation allows us to clearly identify the initial *triggering* Si seed that sits at the opposite side of the original pit. It is also possible for the drawing force on the triple phase line to displace or even break the initial segment of SiNWs away from its initial nucleation seeds.

Meanwhile, inactive catalyst drops (which fail to lead a lateral growth of SiNWs) are also observed. There are generally two situations for these inactive drops: (i) as shown in Fig. 5(a), if the catalyst drop produces simultaneously multiple Si seeds of similar size at the bottom edge line, the forces of the Si seeds to tilt the catalyst drop into one direction cancel each other; (ii) if the growth of the SiNW segment develops in a vertical direction [similar to the VLS growth mode as shown in Fig. 5(b)], the catalyst drop is no more in contact with the a-Si:H on the substrate. In this case, the catalyst drop is unable to reach the nearby a-Si:H layer to form a new absorption front and thus the growth will stop after consuming all of the covering a-Si:H layer. Therefore, the formation of a new absorption front (interface) with the nearby a-Si:H layer that covers the substrate, as illustrated in Fig. 3(c), is the key step for a successful growth of lateral SiNWs. This will, in turn, rely on the formation of *large enough* and *asymmetrically distributed* Si seeds at the catalyst bottom edge to effectively tilt/trigger the catalyst drop into one specific growth direction.

Considering that the nucleation of Si seeds in the catalyst relies on the supply of Si atoms from the a-Si:H layer to build up a supersaturation concentration of dissolved Si atoms in the catalyst, with respect to a-Si/In interface $C^a_{eq} = C^c_{eq} \cdot e^{\Delta E_{ac}/kT}$, a critical thickness of the a-Si:H covering thin layer needs to be absorbed. Since the solubility of Si in In (Ref. 19) is much lower as compared to that in Au (Ref. 20) and Cu,[21] much less Si atoms have to be absorbed in order to

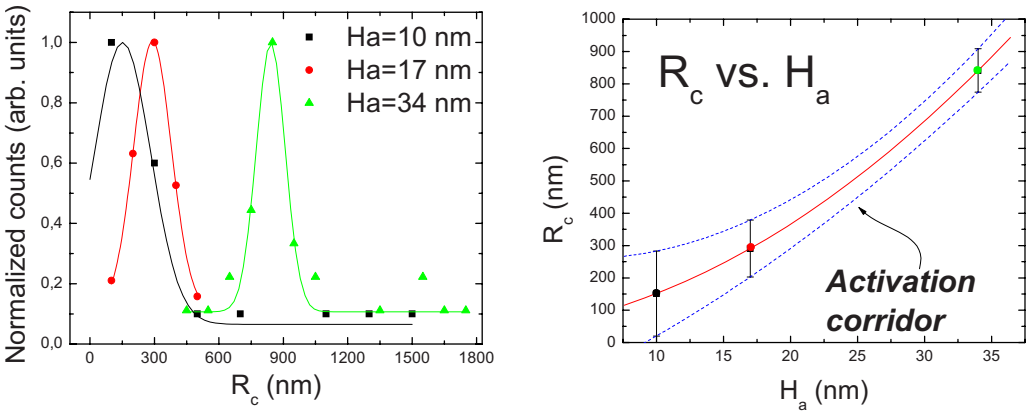


FIG. 6. (Color online) (a) Statistics on the dependence of the successful growth of lateral SiNWs on the diameter of the In catalyst drops ($s$), for various a-Si:H covering thickness ($H_a$): 10, 17, and 34 nm. (b) The data in (a) are replotted with the size of the active catalyst as a function of the thickness of the a-Si:H covering layer. The FWHM of the distributions in (a) are used to define an activation corridor for achieving a high activation rate of lateral SiNWs.

establish supersaturation in the In catalyst. The critical thickness for establishing an initial supersaturation (of $C_{eq}^{a}$) in the In catalyst drop is estimated to be

$$\frac{H_a^{ini}\pi R_c^2/\Omega_{\mathrm{Si}}}{(\pi/6)R_c^3/\Omega_{\mathrm{In}}} > C_{eq}^{a} \Rightarrow H_a^{ini} \geq \frac{1}{6}C_{eq}^{c}\cdot e^{\Delta E_{ac}/kT}\cdot \Omega_{\mathrm{Si}}/\Omega_{\mathrm{In}}\cdot R_c \sim 10^{-3}\cdot R_c, \quad (6)$$

with $\Omega_{\mathrm{Si}}$, $\Omega_{\mathrm{In}}$, and $R_c$ being the atomic volume of Si and In atoms and the diameter of the In catalyst drop, respectively. $H_a^{ini}$ is usually less than $<1$ nm for typical catalyst drops of 200–500 nm (at 500 °C). However, this is far less than the thickness required for the formation of large Si seed(s) to effectively tilt the catalyst, which will require continuous absorption of Si atoms from the a-Si:H covering layer. If the volume ratio of the largest Si seed to the catalyst drop is roughly of $\sigma_v = V_{seed}/V_c \sim 0.02$ (for typical catalyst drops in range of 300–500 nm according to SEM observations), with $V_{seed}$ and $V_c$ being the volume of the Si seed and catalyst drop, a minimum thickness of the a-Si:H covering layer for the nucleation and growth of the large Si seed(s) is required

$$H_a^{nc}\pi\cdot R_c^2\cdot\alpha/(\pi/6\cdot R_c^3) \geq m\cdot\sigma_v \Rightarrow H_a^{nc} \geq \frac{m\cdot\sigma_v}{3\alpha}R_c \sim 10^{-2}\cdot R_c, \quad (7)$$

where $m \geq 1$ is the number of coexisting Si seeds of similar size and $\alpha$ is a geometry constant that accounts for the volume contraction between amorphous and crystalline Si.

According to the statistics on the successful growth of SiNWs, it is the ratio of the covering a-Si:H thickness ($H_a$) to the diameter of the catalyst ($R_c$) that determines the activation rate of the catalyst drops for the growth of lateral SiNWs. A series of three samples were prepared with different a-Si:H covering thickness of 10, 17, and 34 nm but with the same $H_2$ plasma treatment and annealing temperature of 450 °C. For each condition, 30–40 active catalyst drops (leading the lateral growth of SiNWs) were sampled by using SEM characterizations to produce the statistics data. As shown in Fig. 6(a), the most likely size for an active catalyst drop shifts from around 151 to 841 nm with the increase in covering a-Si:H thickness. The data in Fig. 6(a) are replotted in Fig. 6(b) with the size of the active catalyst as a function of the thickness of the a-Si:H covering layer. Moreover, we use the full width at half maximum (FWHM) of the distribution fittings in Fig. 6(a) to define a region for which the growth of the IPSLS SiNW will most likely take place. As depicted in Fig. 6(b), we identify this region as an *activation corridor* for achieving a high activation rate of the lateral SiNWs.

As can also be seen in Fig. 6(b), a too thick a-Si:H layer (for a given catalyst size) is unfavorable for the growth of IPSLS SiNWs. This can be understood based on the fact that in order to form a new absorption front/interface with the nearby a-Si:H layer, the catalyst drop needs to emerge out of the covering a-Si:H shell, which is solid in the temperature range of experiment. The influence of the Si seeds on the catalyst drop will be limited by the solid shell. Before the full consumption of the solid a-Si:H covering shell, the movement of the catalyst drop (guided by the contact interface with the a-Si:H shell) is basically vertical since the forces in lateral direction cancel each other for a hemispherical catalyst. So, with a too thick a-Si:H layer, the catalyst will most likely produce multiple Si seeds around the bottom edges or grow in a basically vertical way before emerging out of the a-Si:H layer. This will detach the catalyst drop from substrate and limit the chance for the catalyst to form a new absorption interface with the nearby a-Si:H layer. Therefore, a suitable thickness of a-Si:H layer should (i) provide enough Si atoms for the formation of large enough Si seeds and (ii) allow for the catalyst to quickly emerge out of the solid a-Si:H shell to form a new absorption interface with the nearby a-Si:H layer, as illustrated in Figs. 3(c) and 3(d).

Besides the general trend shown in Fig. 6, there are also some exceptional cases for very large catalyst drops, which

are active even in a range far away from the activation corridor, as can be seen in Fig. 6(a). This could be explained, for example, by considering that there is just one *dominant* Si seed formed along the bottom edge. This seed would collect most of the dissolved Si atoms in the catalyst while the larger surface area of the catalyst drop (proportional to $\sim R_c^2$) would enable this *lucky* Si seed to grow into a size large enough to tilt the catalyst drop. However, further investigation about this point is still needed.

In summary, we have presented a comprehensive investigation of the initial nucleation and growth of IPSLS SiNWs. The major growth steps and the underlying mechanism have been discussed. A successful activation of the catalyst drop for the SiNWs growth relies on the formation of a new absorption interface with the nearby a-Si:H layer. The ratio of the covering a-Si:H thickness to the diameter of the catalyst is identified as the key parameter for achieving a high growth activation of the IPSLS-SiNWs, which provides important information for understanding the initial stage of the IPSLS-SiNWs and lays a basis for their future device applications.

[1] R. S. Wagner and W. C. Ellis, Appl. Phys. Lett. **4**, 89 (1964).
[2] N. Wang, Y. H. Tang, Y. F. Zhang, C. S. Lee, and S. T. Lee, Phys. Rev. B **58**, R16024 (1998).
[3] Y. Huang, X. Duan, Q. Wei, and C. M. Lieber, Science **291**, 630 (2001).
[4] Y. Cui, Z. Zhong, D. Wang, W. U. Wang, and C. M. Lieber, Nano Lett. **3**, 149 (2003).
[5] J. F. Hsu, B. R. Huang, C. S. Huang, and H. L. Chen, Jpn. J. Appl. Phys., Part 1 **44**, 2626 (2005).
[6] Y. Cui, Q. Q. Wei, H. K. Park, and C. M. Lieber, Science **293**, 1289 (2001).
[7] L. Tsakalakos, J. Balch, J. Fronheiser, B. A. Korevaar, O. Sulima, and J. Rand, Appl. Phys. Lett. **91**, 233117 (2007).
[8] Th. Stelzner, M. Pietsch, G. Andr, F. Falk, E. Ose, and S. Christiansen, Nanotechnology **19**, 295203 (2008).
[9] L. Yu, P.-J. Alet, G. Picardi, and P. Roca i Cabarrocas, Phys. Rev. Lett. **102**, 125501 (2009).
[10] S. Roorda, S. Doorn, W. C. Sinke, P. M. L. O. Scholte, and E. van Loenen, Phys. Rev. Lett. **62**, 1880 (1989).
[11] I. Stich, R. Car, and M. Parrinello, Phys. Rev. B **44**, 11092 (1991).
[12] G. L. Olson and J. A. Roth, Mater. Sci. Rep. **3**, 1 (1988).
[13] N. Bernstein, M. J. Aziz, and E. Kaxiras, Phys. Rev. B **61**, 6696 (2000).
[14] S. Kodambaka, J. Tersoff, M. C. Reuter, and F. M. Ross, Phys. Rev. Lett. **96**, 096105 (2006).
[15] W. A. Tiller, *The Science of Crystallization: Microscopic Interfacial Phenomena* (Cambridge University Press, New York, 1991).
[16] V. G. Dubrovskii, N. V. Sibirev, G. E. Cirlin, J. C. Harmand, and V. M. Ustinov, Phys. Rev. E **73**, 021603 (2006).
[17] J. Kühnle, R. B. Bergmann, and J. H. Werner, J. Cryst. Growth **173**, 62 (1997).
[18] Z. Z. You, J. Electron Spectrosc. Relat. Phenom. **160**, 29 (2007).
[19] C. D. Thurmond, J. Phys. Chem. **57**, 827 (1953).
[20] E. I. Givargizov, J. Cryst. Growth **31**, 20 (1975).
[21] J. Arbiol, B. Kalache, P. Roca i Cabarrocas, J. R. Morante, and A. Fontcuberta i Morral, Nanotechnology **18**, 305606 (2007).